Mechanistic studies of cancer cell mitochondria- and NQO1-mediated redox activation of beta-lapachone, a potentially novel anticancer agent

By: Jason Z. Li, Yuebin Ke, Hara P. Misra, Michael A. Trush, Y. Robert Li, Hong Zhu, Zhenquan Jia

Jason Z. Li, Yuebin Ke, Hara P.Misra, Michael A. Trush, Y. Robert Li, Hong Zhud, Zhenquan Jia. (2014). Mechanistic studies of cancer cell mitochondria- and NQO1-mediated redox activation of beta-lapachone, a potentially novel anticancer agent. *Toxicology and Applied Pharmacology, 281(3), 285-293.* doi:10.1016/j.taap.2014.10.012

Abstract:

Beta-lapachone (beta-Lp) derived from the Lapacho tree is a potentially novel anticancer agent currently under clinical trials. Previous studies suggested that redox activation of beta-Lp catalyzed by NAD(P)H:quinone oxidoreductase 1 (NQO1) accounted for its killing of cancer cells. However, the exact mechanisms of this effect remain largely unknown. Using chemiluminescence and electron paramagnetic resonance (EPR) spin-trapping techniques, this study for the first time demonstrated the real-time formation of ROS in the redox activation of beta-lapachone from cancer cells mediated by mitochondria and NQO1 in melanoma B16–F10 and hepatocellular carcinoma HepG2 cancer cells. ES936, a highly selective NQO1 inhibitor, and rotenone, a selective inhibitor of mitochondrial electron transport chain (METC) complex I were found to significantly block beta-Lp meditated redox activation in B16–F10 cells. In HepG2 cells ES936 inhibited beta-Lp-mediated oxygen radical formation by ~ 80% while rotenone exerted no significant effect. These results revealed the differential contribution of METC and NQO1 to beta-lapachone-induced ROS formation and cancer cell killing. In melanoma B16–F10 cells that do not express high NQO1 activity, both NOQ1 and METC play a critical role in beta-Lp redox activation. In contrast, in hepatocellular carcinoma HepG2 cells expressing extremely high NQO1 activity, redox activation of beta-Lp is primarily mediated by NQO1 (METC plays a minor role). These findings will contribute to our understanding of how

cancer cells are selectively killed by beta-lapachone and increase our ability to devise strategies to enhance the anticancer efficacy of this potentially novel drug while minimizing its possible adverse effects on normal cells.

Abbreviations

- beta-Lp, beta-lapachone;
- CL, chemiluminescence;
- DCF, dichlorodihydrofluoroscein;
- DCIP,dichloroindophenol;
- DEPMPO, 5-(Diethoxyphosphoryl)-5-methyl-1-pyrroline-N-oxide;
- DMEM, Dulbecco's modified Eagle's medium;
- DMPO, 5,5-dimethyl-1-pyrroline N-oxide;
- EPR, electron paramagnetic resonance;
- FBS, fetal bovine serum;
- HRP, horseradish peroxidase;
- METC, mitochondrial electron transport chain;
- NQO1, NAD(P)H:quinone oxidoreductase 1;
- PBS, phosphate-buffered saline;
- ROS,reactive oxygen species;
- SOD, superoxide dismutase

Keywords: Beta-lapachone | NQO1 | ROS | Mitochondrial electron transport chain | EPR | Cancer cells

Article:

Introduction

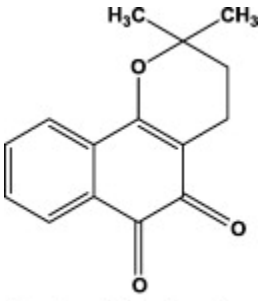

Structure of beta-lapachone

Cancer is one of the major causes of death worldwide. Currently, there is no cure for the large majority of cancers, and as such, development of effective anticancer drugs is of urgent clinical importance. In this context, beta-lapachone (beta-Lp), a quinone compound derived from Lapacho tree, has been shown to be highly effective in treating various types of cancer in experimental models, including liver cancer and melanoma (Blanco et al., 2010, Brightman et

al., 1992, Dong et al., 2009, Pardee et al., 2002 and Reinicke et al., 2005). This novel agent is also currently under clinical trials for treating cancer patients (Trachootham et al., 2009).

Although beta-Lp is a promising anticancer agent, its mechanisms of action still need to be fully elucidated. The leading theory holds that beta-Lp reacts with the cellular enzyme NAD(P)H:quinone oxidoreductase 1 (NQO1), which is overexpressed in many cancers, leading to a futile cycling between its quinone and hydroquinone forms, thereby consuming NADPH and generating reactive oxygen species (ROS) (Pink et al., 2000 and Siegel et al., 2012). It is suggested that depletion of NADPH may trigger cancer cell apoptosis. In addition, formation of ROS from redox cycling of beta-Lp may also contribute to its cancer cell killing activity (Pink et al., 2000 and Siegel et al., 2012). Also, current theories seem to agree on the importance of NQO1 in the anticancer action of beta-Lp, especially in cancer cells that express high NQO1 activity (Pink et al., 2000 and Siegel et al., 2012). In most of the experiments verifying NQO1 as the principal cellular factor, the NQO1 inhibitor dicumarol was used (Bey et al., 2007, Li et al., 2011 and Pardee et al., 2002). Dicumarol, however, is also a mitochondrial inhibitor (Gonzalez-Aragon et al., 2007), making it difficult to delineate the exact role of NQO1 in redox activation of beta-Lp. Moreover, the involvement of other cellular factors in redox activation of beta-Lp in cancer cells that do not express high NQO1 activity and the subsequent real-time formation of ROS remain unknown. Unlike those in normal cells, mitochondria in cancer cells are extremely inefficient in generating ATP, which provides energy for cellular work, in part because of excessive electron leakage in the electron transport chain (Enns and Ladiges, 2012 and Lu et al., 2012). We hypothesized that leaked electrons from mitochondrial electron transport chain (METC) may also play a role in redox activation of beta-Lp and thus the generation of ROS, particularly in cancer cells that do not express high NQO1 activity. Using melanoma and hepatocellular carcinoma cell lines and selective NQO1 and mitochondrial inhibitors as well as purified NQO1 enzyme and isolated mitochondria, we for the first time demonstrated real-time formation of ROS from cancer cell mitochondria- and NQO1-mediated redox activation of beta-Lp and revealed the differential contribution of METC and NQO1 to beta-Lp-induced ROS formation and cancer cell killing. These findings may significantly contribute to our understanding of how beta-Lp becomes redox activated to selectively kill cancer cells and may thus increase our ability to develop strategies to enhance its cancer killing activity while minimizing its potential adverse effects on normal cells.

Materials and methods

Materials

B16–F10 melanoma and hepatocellular carcinoma HepG2 cell lines were from ATCC (Manassas, VA). Dulbecco's modified Eagle's medium (DMEM), penicillin, streptomycin, fetal bovine serum (FBS), and phosphate-buffered saline (PBS) were from Invitrogen (Carlsbad, CA). Cell culture flasks and other plastic wares were from Corning (Corning, NY). The specific NQO1 inhibitor ES936 was a gift from Dr. David Ross (University of Colorado, Denver). The

spin traps 5-(Diethoxyphosphoryl)-5-methyl-1-pyrroline-*N*-oxide (DEPMPO) and 5,5-dimethyl-1-pyrroline *N*-oxide (DMPO) were from Enzo (Farmingdale, NY). Recombinant human NQO1 was from MyBioSource (San Diego, CA). All other chemicals/agents were from Sigma (St. Louis, MO).

Cell culture

B16–F10 and HepG2 cells were cultured in DMEM supplemented with 10% FBS, 100 U/ml penicillin and 100 μg/ml streptomycin at 37 °C in a humidified atmosphere of 5% CO_2.

Isolation of mitochondria

Mitochondria were isolated from freshly harvested B16–F10 cells by differential centrifugation method described before (Zhu et al., 2009). Briefly, cells were washed once with PBS and centrifuged. The cell pellet was resuspended in 5 ml sucrose buffer (0.25 M sucrose, 10 mM Hepes, 1 mM EGTA and 0.5% BSA, pH 7.4), homogenized in a Dounce tissue grinder on ice. The homogenate was centrifuged at 1500 *g* for 10 min at 4 °C. The supernatant was collected and centrifuged at 10,000 *g* for 10 min at 4 °C. The resulting mitochondrial pellet was washed twice with sucrose buffer and then resuspended in ice-cold 50 mM potassium phosphate buffer, pH 7.0, containing 1 mM EDTA and 0.1% Triton X-100, followed by sonication to lyse the mitochondria. The resulting mitochondrial pellet was washed twice with sucrose buffer and kept on ice for ROS measurement (see below).

NQO1 activity assay

Cellular NQO1 activity was determined using dichloroindophenol (DCIP) as the two-electron acceptor, as described before (Zhu et al., 2009). The dicumarol-inhibitable cellular NQO1 activity was calculated using the extinction coefficient of 21.0 mM^{-1} cm^{-1}, and expressed as nanomoles of DCIP reduced per minute per milligram of cellular protein.

Oxygen consumption assay

The rate of O_2 consumption by cancer cells was measured polarographically with a Clark-type O_2 electrode at 37 °C in 2.5 ml complete PBS, as described before (Li and Trush, 1998). For measuring O_2 consumption stimulated by beta-Lp redox cycle, 0.2 mM KCN was added to inhibit mitochondrial respiration before adding beta-Lp to the cell suspension.

Chemiluminescence (CL) assays

Chemiluminescence (CL) assays are best known for their remarkable sensitivity in detecting cellular ROS in various biological systems as previously described by us and others (Li and Trush, 1998, Li et al., 1998, Li et al., 1999a and Li et al., 1999b). In this context, lucigenin-amplified CL assay has been used to sensitively detect biological superoxide generation. On the other hand, luminol-amplified CL in the present of horseradish peroxidase (HRP) has been used

to sensitively detect H_2O_2 formation in cells and isolated mitochondria (Li and Trush, 1998, Li et al., 1998, Li et al., 1999a and Li et al., 1999b). For detecting cellular ROS formation, CL was continuously measured with a Berthold LB9505 luminometer at 37 °C upon mixing the cells (1×10^6/ml) with lucigenin (20 μM) or luminol (10 μM) plus HRP (10 μg/ml) in complete PBS. For measuring mitochondrial H_2O_2 release, CL was measured in the same manner as described above upon mixing mitochondria (0.05 mg/ml) with 0.5 mM pyruvate and 0.5 mM malate (to provide NADH for the mitochondrial electron transport chain) in respiration buffer.

Electron paramagnetic resonance (EPR) assay

For spin-trapping measurement of oxygen radicals, EPR spectra were recorded at room temperature with a spectrometer (E-Scan, Bruker), operating at X-band with a TM cavity, as described previously (Zang and Misra, 1993). For measuring cellular oxygen radical formation, cells (1×10^6/ml) containing 10 μM Fe^{2+} in complete PBS were incubated with 80 mM DMPO in the presence or absence of beta-Lp at 37 °C for 5 min before being subject to EPR measurement. The EPR spectrometer settings of DMPO spin trapping measurement were: modulation frequency, 100 kHz; X-band microwave frequency, 9.5 GHz; microwave power, 15 mW (milliwatts); modulation amplitude, 1.0 G (gauss); time constant, 160 s; scan time, 200 s; and receiver gain, $1 \times l0^5$. For measuring oxygen radical formation by isolated mitochondria, mitochondria (0.05 mg/ml) were incubated with 25 mM DEPMPO in respiration buffer in the presence or absence of beta-Lp at 37 °C for 5 min before being subject to EPR measurement. For measuring oxygen radical formation from purified NQO1-catalyzed redox cycling of beta-Lp, NQO1 (0.5 μg/ml) was incubated with 0.25 mM NADPH and 25 mM DEPMPO in complete PBS in the presence or absence of beta-Lp at 37 °C for 5 min before being subject to EPR measurement. The EPR spectrometer settings of DEPMPO spin trapping measurement were: modulation frequency, 100 kHz, X band microwave frequency, 9.5 GHz; microwave power, 20 mW (milliwatts); modulation amplitude, 1 G (gauss); time constant, 160 s; scan time, 50s; and receiver gain, $5 \times l0^5$.

Spectrophotometric assay for NADPH consumption

Measurement of NADPH was determined using methods as described previously (Brightman et al., 1992). In brief, cells were first washed with DMEM medium without phenol red, pH 7.4. NADPH consumption was monitored continuously at 340 nm using a Beckman Coulter DU 800 spectrophotometer for 5 min at 37 °C upon mixing NQO1 (0.5 μg/ml) with 25 mM NADPH in complete PBS in the presence or absence of beta-Lp.

Cytotoxicity assay and microscopic examination

Cell viability was determined by MTT assay as described before (Mosmann, 1983). In brief, cells (2×10^5cells/well in 0.5 ml culture medium) were plated into 24-well tissue culture plates. After incubation of the cells with beta-Lp in DMEM supplemented with 0.5% FBS at 37 °C for 24 h, the morphological changes were examined under an inverted phase contrast microscope

and photographed using a Nikon Digital Sight camera with NIS Elements D3 software. Then, 50 μl of MTT (2 mg/ml PBS) was added to each well followed by 2-hr incubation at 37 °C. The reduction of MTT to formazan by viable cells was detected at 570 nm. Cell viability was expressed as percentage of MTT reduction in control cells.

Statistical analysis

All data are expressed as mean ± SD from at least three separate experiments unless otherwise indicated. Differences between the mean values of multiple groups were analyzed by one-way analysis of variance followed by Student–Newman–Keuls test. Differences between the 2 groups were analyzed by Student *t*-test. Statistical significance was considered at $p < 0.05$.

Results and discussion

Selection and characterization of melanoma B16–F10 and hepatocellular carcinoma HepG2 cells

Cell culture models are crucial for understanding the biology of cancer cells as well as the action of anticancer drugs. In this study, mouse melanoma B16–F10 and human hepatocellular carcinoma HepG2 cell lines were selected because metastatic melanoma and hepatocellular carcinoma are among the cancers with poor prognosis and that lack effective therapies (Neuzillet et al., 2014, Tronnier and Mitteldorf, 2014 and Villanueva et al., 2013). In addition, B16–F10 cells were derived from C57BL/6 mice, and the cells can be implanted into the mice to serve as a commonly used in vivo model for cancer research (Kayaga et al., 1999, Lentini et al., 2012 and Shao et al., 2001). As shown in Fig. 1A, both B16–F10 and HepG2 cells exhibited similar mitochondrial respiration as assessed by KCN-sensitive O_2 consumption. However, B16–F10 cells showed higher mitochondrial superoxide production than HepG2 cells, as detected by lucigenin-derived CL (Fig. 1B), suggesting that mitochondrial electron transport chain (METC) in B16–F10 cells may be more leaky than that in HepG2 cells. It has been proposed that mitochondria in cancer cells, especially those with high metastatic potential, produce more ROS than those in normal cells, and the basal ROS formation may play a role in maintaining malignant phenotype (Enns and Ladiges, 2012, Ishii, 2007, Kamat and Devasagayam, 2000, Ralph et al., 2010, Singh, 2006, Wallace, 2005 and Wenner, 2012). Indeed, B16–F10 cells are much more metastatic than HepG2 cells (Wu et al., 2009). Whether the elevated basal production of mitochondrial superoxide plays a role in melanoma metastasis warrants further investigation. Notably, although HepG2 cells showed lower basal mitochondrial superoxide production, these cells contained a much higher level (> 40-fold) of NQO1 than B16–F10 cells (Fig. 1C). The differences in mitochondrial activity and NQO1 levels in these 2 cancer cell lines make them useful in vitro models for studying the mechanistic roles of mitochondria and NQO1 in redox activation of beta-Lp to lead to cancer cell killing.

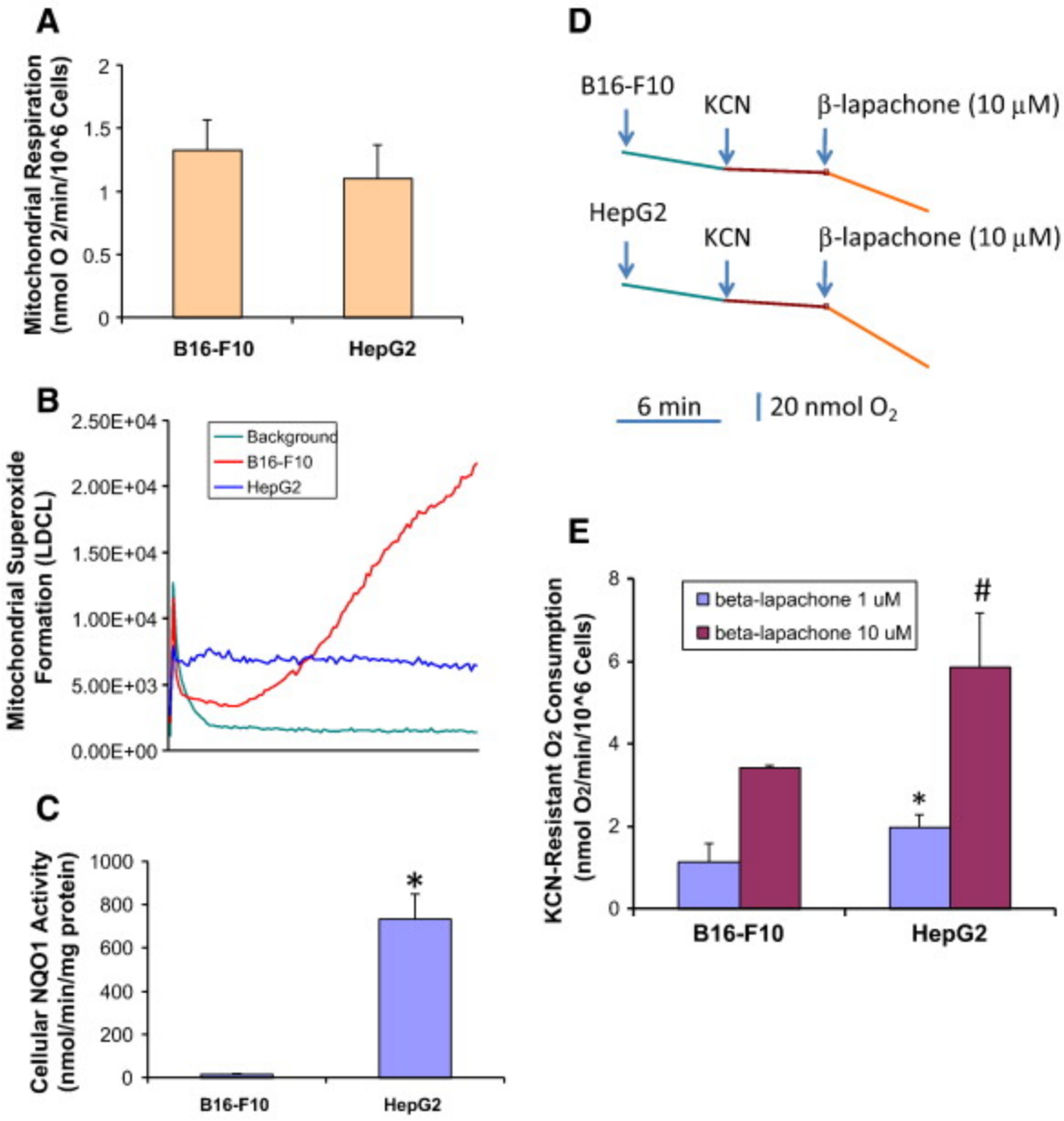

Fig. 1. Mitochondrial and NQO1 activities, and KCN resistant oxygen consumption in melanoma B16–F10 cells and hepatocellular carcinoma HepG2 cells. Panel A shows KCN-sensitive cellular oxygen consumption indicating mitochondrial respiration; panel B shows mitochondrial superoxide production detected by lucigenin-derived CL (LDCL) in the cancer cells; lucigenin concentration is 20 μM. Panel C shows NQO1 activity as measured by dicumarol-inhibitable reduction of DCIP. Panels D–E show beta-Lp redox cycling as determined by KCN-resistant O_2 consumption. Values are mean ± SEM, n = 3. *, $p < 0.05$ as compared with B16–F10 cells (panel C). *$p < 0.05$ compared with beta-lapachone 1 μM in B16–F10 cells (panel E); #$p < 0.05$ compared with beta-lapachone 10 μM in B16–F10 cells (panel E).

Evidence for redox cycling of beta-Lp in cancer cells

Although it has been claimed in the literature that beta-Lp may undergo futile redox cycling in cancer cell, direct evidence is still lacking. Hence, we decided to first use KCN-resistant O_2 consumption assay to determine the redox cycling property of this compound in both B16–F10 and HepG2 cells. KCN-resistant O_2consumption is widely accepted as a gold-standard assay for determining chemical redox cycling. As shown in Figs. 1D–E, addition of beta-Lp to the cancer cells resulted in marked KCN-resistant O_2 consumption, indicating that beta-Lp is a redox cycler in both types of cancer cells. Notably, beta-Lp stimulated more KCN-resistant O_2 consumption in HepG2 cells than in B16–F10 cells, suggesting more potent redox activation of beta-Lp in HepG2 cells. This is in line with the data showing that HepG2 cells expressed a much higher level of NQO1 than B16–F10 cells (Fig. 1C).

Formation of ROS from redox cycling of beta-Lp in cancer cells

As stated in the Introduction section, redox cycling of beta-Lp may lead to depletion of NADPH and generation of ROS (Pink et al., 2000). However, evidence showing real-time formation of ROS from redox activation of beta-Lp in cancer cells is lacking. There is only one published article showing that beta-Lp stimulated dichlorodihydrofluoroscein (DCF) fluorescence (Park et al., 2011), an assay for overall oxidative stress. However, DCF assay suffers major limitations, including its non-specificity for ROS. In this regard, metal ions and peroxidase are able to oxidize DCF to form fluorescent product (Rota et al., 1999). In view of the above, we used the highly sensitive chemiluminescence assay and the most specific EPR spin-trapping technique to determine the ROS formation from beta-Lp redox activation in cancer cells. Fig. 2 showed the real-time formation of cellular H_2O_2 as detected by luminol CL in the presence of HRP. In data not shown, this CL response was blocked by adding catalase, proving that the CL response was indicative of H_2O_2formation. The formation of cellular H_2O_2 from beta-Lp redox activation was concentration-dependent in both types of cancer cells. Notably, the kinetics of H_2O_2 formation in HepG2 cells was much faster than that in B16–F10 cells (Figs. 2A, B). Integrated CL which is indicative of the total amounts of H_2O_2 formed over 30 min showed that beta-Lp produced more H_2O_2 in HepG2 cells than in B16–F10 cells (Figs. 2C, D). This observation was in agreement with the data shown earlier (Fig. 1) that redox cycling of beta-Lp occurred more rigorously in HepG2 cells than in B16–F10 cells. The more rapid kinetics and higher amounts of H_2O_2formation in HepG2 cells were also in line with the data showing that HepG2 cells expressed 40-fold higher NQO1 activity than B16–F10 cells (Fig. 1C).

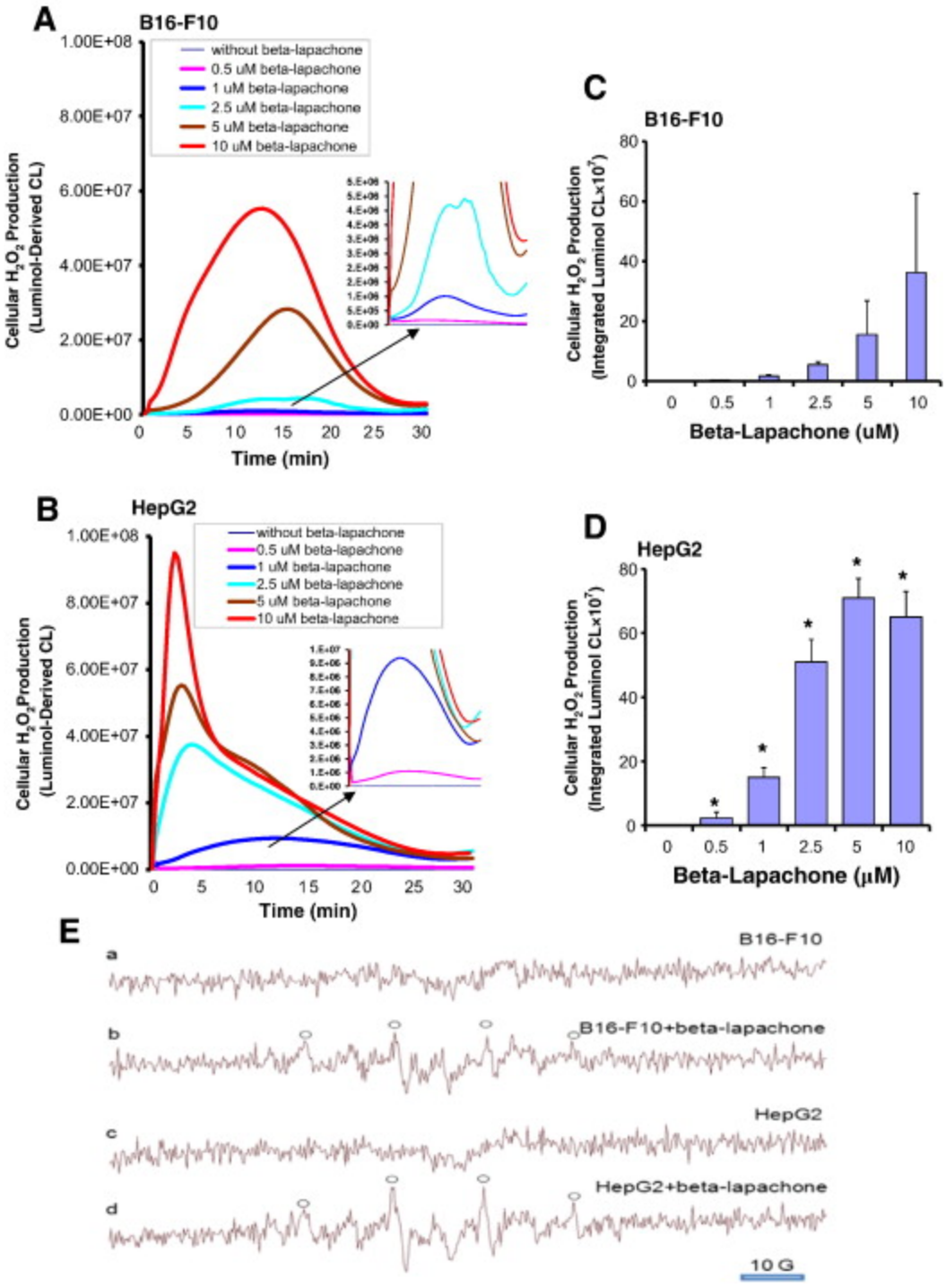

Fig. 2. Real-time and accumulated formation of reactive oxygen species (ROS) from beta-Lp redox activation in cancer cells detected by luminol/HRP-dependent CL and EPR. Real time formation of ROS from beta-lapachone redox cycling was detected by time-dependent luminol CL in the presence of HRP in melanoma B16–F10 cells (panel A) and hepatocellular carcinoma HepG2 cells (panel B). Integrated luminol CL in the presence of HRP in melanoma B16–F10 cells (panel C) and hepatocellular carcinoma HepG2 cells (panel D) was measured in 30 min in

the presence of HRP from beta-lapachone redox cycling. Panel E shows the formation of hydroxyl radicals from beta-Lp (10 μM) redox activation detected by EPR DMPO (80 mM) spin-trapping in B16–F10 (lanes a–b) and HepG2 (lanes c–d) cells in complete PBS. In data not shown, the luminol/HRP-dependent CL response was completely blocked by adding catalase (250 U/ml), indicating that this assay under the conditions described in this study measures H_2O_2 released from the cancer cells. Values are mean ± SEM, n = 3. *, $p < 0.05$ versus control HepG2 cells.

EPR spin-trapping was further employed to detect oxygen radical formation by beta-Lp in cancer cells. As shown in Fig. 2E, incubation of cancer cells with beta-Lp led to the formation of DMPO-OH adduct with $a_N = a_H = 14.9$ G, indicating hydroxyl radical formation. DMPO has been widely used as a good candidate for spin trapping agent to study the production of reactive free radicals such as hydroxyl radicals in biological systems (Hojo et al., 2000, Liu et al., 1999 and Timmins et al., 1999). However, it was reported that the hydroxyl radical spin-adduct, DMPO-OH could also be derived from the decomposition of the superoxide spin-adduct (DMPO-OOH) (Hojo et al., 2000, Jia et al., 2009, Liu et al., 1999 and Timmins et al., 1999). To further study whether the DMPO-OH was initially derived from DEPMO-OOH, we added 500 U/ml superoxide dismutase (SOD) prior to initiation of the reactions. In data not shown, the intensity of DMPO-OH spectrum was not affected by SOD indicating that the DMPO-OH signal is not mediated by the decomposition of the superoxide spin-adduct (DMPO-OOH), which is consistent with our previous report (Jia et al., 2009). Consistent with the CL data, hydroxyl radical formation in HepG2 cells was also more dramatic than that in B16–F10 cells. Our data for the first time conclusively demonstrated the real-time formation of H_2O_2 as well as the generation of hydroxyl radicals from beta-Lp redox activation in cancer cells.

Role of mitochondrial electron transport chain (METC) and NQO1 in redox activation of beta-Lp to produce ROS in cancer cells

As mentioned in the Introduction section, NQO1 has been suggested to be the principal factor to mediate redox activation of beta-Lp in cancer cells. This conclusion was derived largely from the use of the non-selective NQO1 inhibitor, dicumarol, which also affects mitochondrial activity (Gonzalez-Aragon et al., 2007). To further investigate the exact role of cellular NQO1 in redox activation of beta-Lp, we used ES936, a highly selective and potent NQO1 inhibitor, which could completely inhibit cellular NQO1 at < 1 μM (Dehn et al., 2003). Rotenone, a selective inhibitor of METC complex I (Fang and Beattie, 2002, Genova et al., 1997,Li et al., 1999b and Uyemura et al., 2004) was used to determine the involvement of METC in beta-Lp redox activation. As shown in Figs. 3A, B, redox activation of beta-Lp to generate H_2O_2 (detected by luminol/HRP-dependent CL) was significantly reduced by ES936, rotenone, and dicumarol. Interestingly, on average, ES936 and rotenone each inhibited the H_2O_2 formation by ~ 40%, and dicumarol alone inhibited the H_2O_2formation by ~ 80%. As shown later in Fig. 4C, METC-mediated redox activation by beta-Lp was also inhibited by dicumarol suggesting the dramatic effect of dicumarol on beta-Lp-induced H_2O_2 formation in B16–F10

cells. The above data suggested that in cancer cells like B16–F10 melanoma cells that do not express high NQO1 activity, both NQO1 and METC seemed to play an equally important role in redox activation of beta-Lp to generate ROS. By comparing the effects of ES936 and rotenone on redox activation of beta-Lp at 2 different concentrations (i.e., 1 and 10 μM) (Figs. 3A, B), we found that in B16–F10 cells incubated with 1 μM beta-Lp, rotenone had an inhibitory effect of ~ 45%, whereas ES936 had an inhibitory effect of ~ 32%. When the concentration of beta-Lp was increased to 10 μM, an increased inhibition by ES936 (~ 41%) and a decreased inhibition by rotenone (~ 32%) occurred. This suggested that at lower concentrations, mitochondria might be significantly involved in beta-Lp redox activation to produce ROS. At higher concentrations of beta-Lp, likely due to the limited capabilities of METC, NQO1 seemed to play a more significant role.

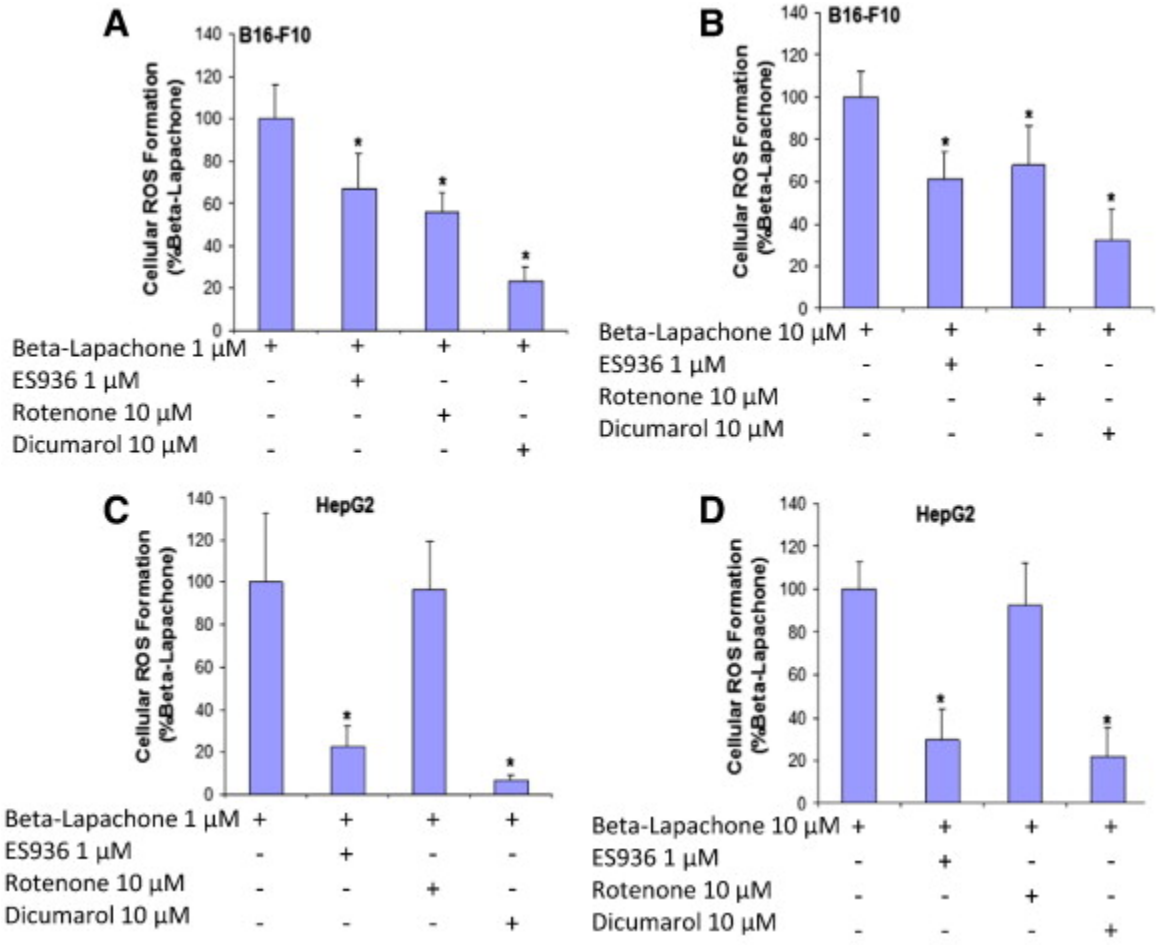

Fig. 3. The roles of mitochondrial electron transport chain (METC) complex I and NQO1 in redox activation of beta-Lp to produce ROS in cancer cells. Dicumarol (10 μM), a non-selective NQO1 inhibitor, ES936 (1 μM), a highly selective and potent NQO1 inhibitor, and rotenone (10 μM), a selective inhibitor of METC complex I were used to determine the involvement of cellular NQO1 and METC complex I in beta-Lp redox activation in B16–F10 (panels A and B) and HepG2 cells (panels C and D), as detected by luminol/HRP-dependent CL. Concentrations

of beta-lapachone are 1 μM (panels A and C) and 10 μM (panels B and D). Values are mean ± SEM, n = 3. *, $p < 0.05$ versus beta-Lp alone.

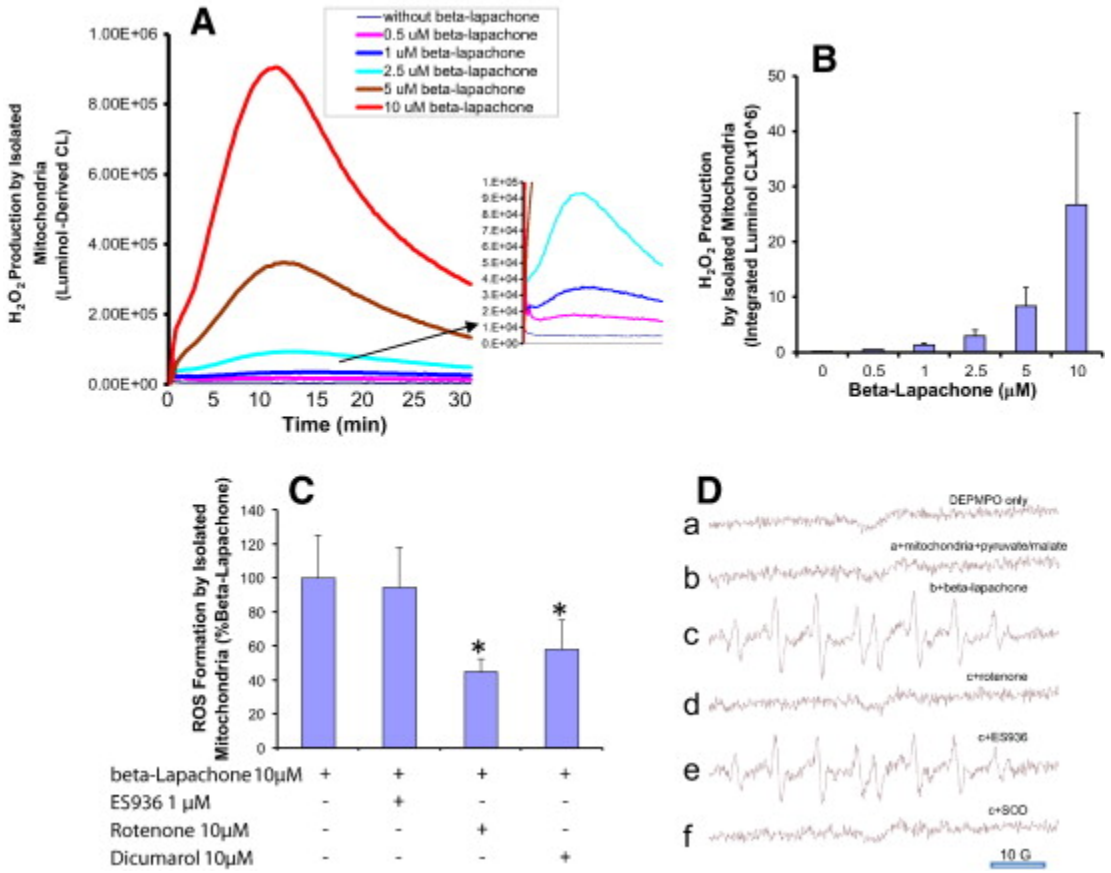

Fig. 4. Detection of ROS in isolated mitochondria by real-time luminol/HRP CL and EPR as well as the involvement of METC/NQO1 in the beta-lapachone redox cycling. Formation of ROS from beta-Lp redox activation in isolated mitochondria driven by pyruvate/malate was measured by luminol CL. (HRP 10 μg/ml; luminol 10 μM). Panel A shows real-time luminol CL response; panel B shows integrated luminol CL for accumulated ROS formation over 30 min. Panel C shows effect of ES936, rotenone, and dicumarol on beta-lapachone induced ROS formation in the isolated mitochondria driven by pyruvate/malate. Panel D shows DEMPO-spin trapping detection of superoxide production from beta-Lp (10 μM) redox cycling in the isolated mitochondria driven by pyruvate/malate. DEPMPO 25 mM; beta-lapachone 10 μM; rotenone 10 μM; ES936 1 μM; SOD 500 U/ml.

As HepG2 cells expressed a 40-fold higher NQO1 activity than B16–F10 cells, we next determined the effects of ES936 as well as rotenone and dicumarol on beta-Lp redox activation in these cells. As shown in Figs. 3C, D, while ES936 and dicumarol each inhibited beta-Lp-mediated H_2O_2 formation by ~ 80% on average, rotenone exerted no significant effect. This data suggested that in cancer cells like HepG2 cells expressing extremely high NQO1 activity,

NQO1-mediated redox activation of beta-Lp seemed to be predominant, and METC appeared to play a very minor, if any, role in the redox activation process.

Studies with isolated mitochondria and purified NQO1

To further prove the involvement of METC and NQO1 in mediating redox activation of beta-Lp to produce ROS, we next used mitochondria isolated from B16–F10 cells and commercially available recombinant human NQO1 enzyme. As shown in Figs. 4A–B, the release of H_2O_2 by pyruvate/malate-driven mitochondria as detected by luminol/HRP-dependent CL was markedly stimulated by beta-Lp in a concentration-dependent manner. Importantly, beta-Lp-stimulated H_2O_2 formation in isolated mitochondria was dramatically inhibited (~ 60%) by rotenone as well as by dicumarol (~ 40% inhibition) (Fig. 4C). This data indicated that METC, especially its complex I was indeed capable of mediating redox activation of beta-Lp. The incomplete inhibition of beta-Lp redox activation by rotenone suggested the possible involvement of other METC complexes in mediating beta-Lp redox activation to form ROS. The marked inhibition of beta-Lp redox activation in isolated mitochondria by dicumarol and the inability of ES936 to do so confirmed that dicumarol is not a selective inhibitor of NQO1, and as such, it should not be used for studying the role of NQO1 in beta-Lp redox activation. On the other hand, our data supported the use of ES936 for such a purpose.

In line with the H_2O_2 formation as detected by luminol/HRP-dependent CL, this study for the first time revealed that beta-Lp stimulated superoxide formation in isolated mitochondria (Fig. 4D). As shown in Fig. 4D, incubation of mitochondria with beta-Lp (10 μM) and DEPMPO (25 mM) led to the generation of a spin-adduct that was completed inhibited by superoxide dismutase (SOD), proving the formation of superoxide. Notably, the production of superoxide was completely blocked by rotenone, but not affected by ES936, again indicating that ES936 at 1 μM did not affect METC, and that its attenuation of cellular ROS formation from beta-Lp redox activation in cancer cells (Fig. 3) was due to the selective inhibition of cellular NQO1. These results with isolated mitochondria further supported a critical role for METC in mediating redox activation of beta-Lp to produce ROS in melanoma B16–F10 cells.

The experiment with purified NQO1 enzyme also proved the ability of NQO1 to catalyze redox activation of beta-Lp to form ROS (Fig. 5). As shown in Fig. 5A, beta-Lp potently stimulated NQO1-catalyzed reaction, leading to the consumption of NADPH in a cell-free system. The consumption of NADPH was completely inhibited by ES936, confirming that the enzymatic activity of NQO1 was essential for catalyzing redox activation of beta-Lp. This study also for the first time demonstrated the formation of oxygen radicals from purified NQO1 enzyme-catalyzed beta-Lp redox activation (Fig. 5B). As shown in Fig. 5B, incubation of NQO1 with 10 μM beta-Lp in the presence of NADPH and DEPMPO led to the formation of a spin-adduct. Although the chemical entity of the spin-adduct remains to be determined, the formation of the spin-adduct was greatly inhibited by SOD, suggesting that this spin-adduct was derived largely from superoxide. The formation of this largely superoxide-dependent adduct was completely inhibited

by ES936, again indicating the dependence of beta-LP redox activation on NQO1 enzymatic activity. Collectively, the results from the experiments with purified NQO1 enzyme proved that NQO1 can directly catalyze redox activation of beta-Lp to produce ROS.

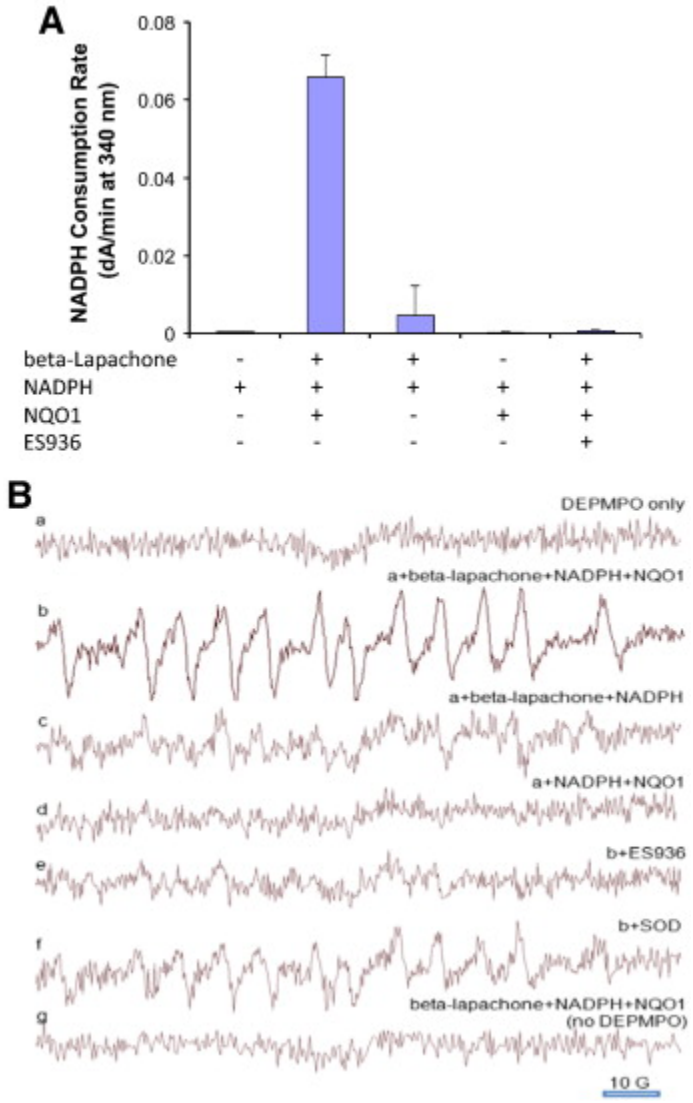

Fig. 5. Beta-lapachone-induced NADPH consumption and EPR detection of superoxide production catalyzed by isolated NQO1. Panel A: Consumption of NADPH (0.25 mM) by NQO1 (0.5 μg/ml) was monitored for 5 min at 340 nm in the presence or absence of Beta-Lp (10 μM) and ES936 (1 μM). Panel B: EPR detection of Beta-Lp (10 μM)-mediated superoxide production catalyzed by NQO1 (0.5 μg/ml). DEPMPO, 25 mM; SOD, 500 U/ml.

Beta-Lp-induced cytotoxicity in cancer cells and the potential involvement of ROS, METC and NQO1 in mediating redox activation of beta-Lp to kill cancer cells

The data presented in Fig. 1, Fig. 2, Fig. 3, Fig. 4 and Fig. 5 collectively showed that beta-Lp underwent mitochondria- and NQO1-mediated redox activation to generate large amounts of

ROS in cancer cells. We next determined the cytotoxicity of beta-Lp in both B16–F10 and HepG2 cancer cells. As shown in Fig. 6, beta-Lp elicited cytotoxicity in both types of cancer cells in a concentration-dependent manner, as assessed by morphologic changes (cells became round and detached) (Fig. 6A) and MTT reduction assay (Fig. 6B). As shown in Fig. 6C, rotenone significantly attenuated beta-Lp cytotoxicity to B16–F10 cells, which once again supported the notion that METC was involved in redox activation of beta-Lp to lead to the death of cancer cells that do not express high NQO1 activity. Notably, beta-Lp was more cytotoxic to HepG2 cells than to B16–F10 cells. This observation was in line with the data showing that beta-Lp underwent more dramatic redox activation to produce higher amounts of ROS in HepG2 cells than in B16–F10 cells (Fig. 1 and Fig. 2). Although HepG2 cells were more sensitive to beta-Lp cytotoxicity, B16–F10 cells expressing very low NQO1 activity were also killed by beta-Lp, especially at 10 μM. Hence, in cancer cells expressing low NQO1 activity beta-Lp still could undergo redox activation, catalyzed by METC in addition to NQO1, to produce ROS that contributed to cancer cell killing. These results may provide novel insights into the molecular and biochemical mechanisms of beta-Lp redox activation in cancer cells to produce ROS that contribute to cancer cell death.

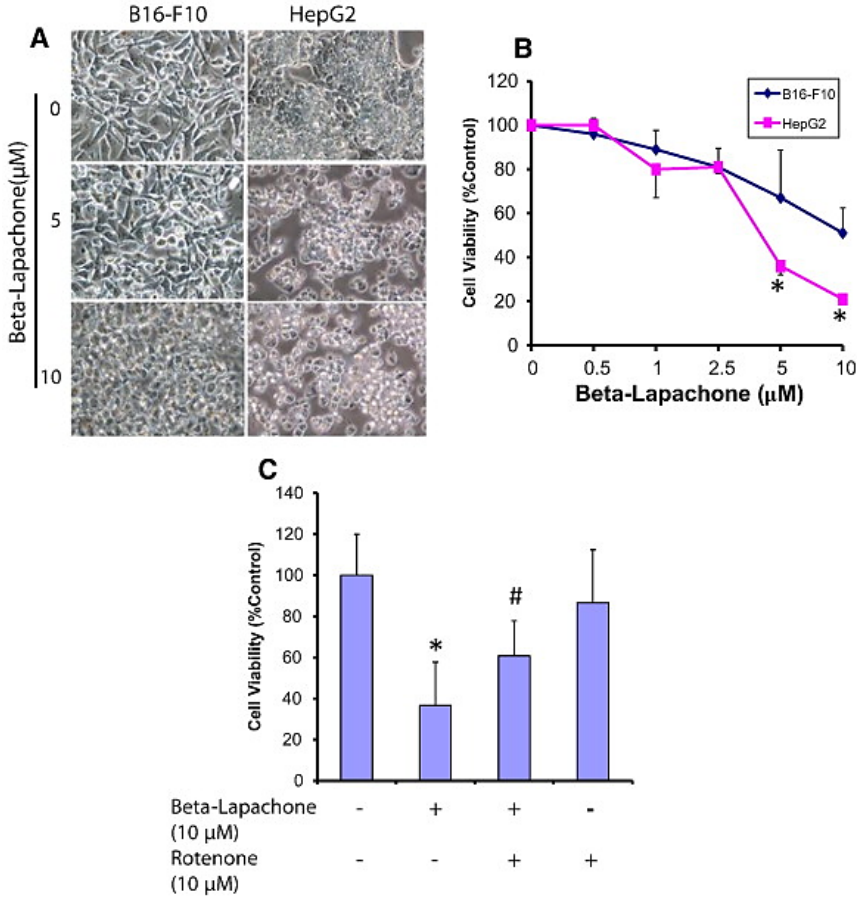

Fig. 6. HepG2 cells expressing high NQO1 are sensitive to beta-lapachone cytotoxicity and effect of rotenone on beta-Lp-induced cytotoxicity in B16–F10 cells. Cells were seeded on 24-

well plates at a density of 2×10^5/well. 24 h later, the cells were treated with the indicated concentrations of beta-lapachone in DMEM containing 0.5% FBS for another 24 h followed by morphological examination (panel A) and MTT assay (panel B). Panel C: the cells were treated with 10 μM beta-lapachone in the presence or absence of rotenone (10 μM) in DMEM containing 0.5% FBS for 24 h followed by MTT assay. *, $p < 0.05$ versus control; #, $p < 0.05$ versus beta-Lp alone (panel D).

The differential roles of cancer cell mitochondria and NQO1 in beta-Lp redox activation reported in this study may significantly contribute to our understanding of how cancer cells are selectively killed by beta-Lp. In this context, future work needs to focus on investigating the detailed molecular and biochemical differences between cancer cells and normal cells with regard to their differential capacities to mediate redox activation of beta-Lp to generate ROS for selective cancer cell killing. Studies are currently underway in our laboratory to compare the redox activation of beta-Lp in human hepatocellular carcinoma HepG2 cells versus in normal human hepatocytes. More experiments are also warranted to further delineate the causal roles of ROS, METC, and cellular NQO1 (both low and high activities) in beta-Lp-induced cancer cell killing as well as in its potential toxicity to normal cells. The mode of cancer cell death (i.e., necrosis, apoptosis, or autophagy) caused by beta-Lp also needs to be determined for further identification of signaling pathways involved in the execution of the cancer cell death following beta-Lp treatment. Since B16–F10 cells used in this study were derived from C57BL/6 mice, investigating the impact of both mitochondria- and NQO1-mediated redox activation of beta-Lp on melanoma growth and metastasis in C57BL/6 mice would provide conclusive evidence on how cancer cells are selectively killed by beta-Lp.

In summary, this study for the first time demonstrated real-time formation of ROS from cancer cell mitochondria- and NQO1-mediated redox activation of beta-Lp in a concentration-dependent manner. In addition, in cancer cells, such as melanoma B16–F10 cells that do not express high NQO1 activity, METC also plays a critical role in beta-Lp redox activation. In contrast, in cancer cells such as hepatocellular carcinoma HepG2 cells expressing extremely high NQO1 activity, redox activation of beta-Lp is primarily mediated by NQO1, and METC plays a minor, if any, role in the redox activation process. We further showed that both isolated mitochondria and purified NQO1 are able to mediate redox activation of beta-Lp to generate ROS. These findings provide the evidence suggesting that the differential roles of mitochondria and NQO1 in mediating redox activation of beta-Lp to produce ROS appear to significantly impact the cancer cell killing activity of this potentially novel anticancer agent.

Conflict of interest

The authors declare that there are no conflicts of interest.

Acknowledgments

This work was supported by a grant from American Institute for Cancer Research grant (09A084).

References

Bey, E.A., Bentle, M.S., Reinicke, K.E., Dong, Y., Yang, C.R., Girard, L., Minna, J.D., Bornmann,

W.G., Gao, J., Boothman, D.A., 2007. An NQO1- and PARP-1-mediated cell death pathway induced in non-small-cell lung cancer cells by beta-lapachone. Proc. Natl. Acad. Sci. U. S. A. 104, 11832–11837.

Blanco, E., Bey, E.A., Khemtong, C., Yang, S.G., Setti-Guthi, J., Chen, H., Kessinger, C.W.,

Carnevale, K.A., Bornmann, W.G., Boothman, D.A., Gao, J., 2010. Beta-lapachone micellar nanotherapeutics for non-small cell lung cancer therapy. Cancer Res. 70, 3896–3904.

Brightman, A.O., Wang, J., Miu, R.K., Sun, I.L., Barr, R., Crane, F.L., Morre, D.J., 1992. A growth factor- and hormone-stimulated NADH oxidase from rat liver plasma membrane. Biochim. Biophys. Acta 1105, 109–117.

Dehn, D.L., Siegel, D., Swann, E., Moody, C.J., Ross, D., 2003. Biochemical, cytotoxic, and genotoxic effects of ES936, a mechanism-based inhibitor of NAD(P)H:quinone oxidoreductase 1, in cellular systems. Mol. Pharmacol. 64, 714–720.

Dong, Y., Chin, S.F., Blanco, E., Bey, E.A., Kabbani, W., Xie, X.J., Bornmann, W.G., Boothman, D.A., Gao, J., 2009. Intratumoral delivery of beta-lapachone via polymer implants for prostate cancer therapy. Clin. Cancer Res. 15, 131–139.

Enns, L., Ladiges, W., 2012. Mitochondrial redox signaling and cancer invasiveness. J. Bioenerg. Biomembr. 44, 635–638.

Fang, J., Beattie, D.S., 2002. Rotenone-insensitive NADH dehydrogenase is a potential source of superoxide in procyclic Trypanosoma brucei mitochondria. Mol. Biochem. Parasitol. 123, 135–142.

Genova, M.L., Bovina, C., Marchetti, M., Pallotti, F., Tietz, C., Biagini, G., Pugnaloni, A., Viticchi, C., Gorini, A., Villa, R.F., Lenaz, G., 1997. Decrease of rotenone inhibition is a sensitive parameter of complex I damage in brain non-synaptic mitochondria of aged rats. FEBS Lett. 410, 467–469.

Gonzalez-Aragon, D., Ariza, J., Villalba, J.M., 2007. Dicoumarol impairs mitochondrial electron transport and pyrimidine biosynthesis in human myeloid leukemia HL-60 cells. Biochem. Pharmacol. 73, 427–439.

Hojo, Y., Okado, A., Kawazoe, S., Mizutani, T., 2000. Direct evidence for in vivo hydroxyl radical generation in blood of mice after acute chromium(VI) intake: electron spin resonance spin-trapping investigation. Biol. Trace Elem. Res. 76, 75–84.

Ishii, N., 2007. Role of oxidative stress from mitochondria on aging and cancer. Cornea 26, S3–S9.

Jia, Z., Zhu, H., Vitto, M.J., Misra, B.R., Li, Y., Misra, H.P., 2009. Alpha-lipoic acid potently inhibits peroxynitrite-mediated DNA strand breakage and hydroxyl radical formation: implications for the neuroprotective effects of alpha-lipoic acid. Mol. Cell. Biochem. 323, 131–138.

Kamat, J.P., Devasagayam, T.P., 2000. Oxidative damage to mitochondria in normal and cancer tissues, and its modulation. Toxicology 155, 73–82.

Kayaga, J., Souberbielle, B.E., Sheikh, N., Morrow, W.J., Scott-Taylor, T., Vile, R., Chong, H., Dalgleish, A.G., 1999. Anti-tumour activity against B16–F10 melanoma with a GMCSF secreting allogeneic tumour cell vaccine. Gene Ther. 6, 1475–1481.

Lentini, A., Tabolacci, C., Nardi, A., Mattioli, P., Provenzano, B., Beninati, S., 2012. Preclinical evaluation of the antineoplastic efficacy of 7-(2-hydroxyethyl)theophylline on melanoma cancer cells. Melanoma Res. 22, 133–139.

Li, Y., Trush, M.A., 1998. Diphenyleneiodonium, an NAD(P)H oxidase inhibitor, also potently inhibits mitochondrial reactive oxygen species production. Biochem. Biophys. Res. Commun. 253, 295–299.

Li, Y., Zhu, H., Kuppusamy, P., Roubaud, V., Zweier, J.L., Trush, M.A., 1998. Validation of lucigenin (bis-N-methylacridinium) as a chemilumigenic probe for detecting superoxide anion radical production by enzymatic and cellular systems. J. Biol. Chem. 273, 2015–2023.

Li, Y., Stansbury, K.H., Zhu, H., Trush, M.A., 1999a. Biochemical characterization of lucigenin (Bis-N-methylacridinium) as a chemiluminescent probe for detecting intramitochondrial superoxide anion radical production. Biochem. Biophys. Res. Commun. 262, 80–87.

Li, Y., Zhu, H., Trush, M.A., 1999b. Detection of mitochondria-derived reactive oxygen species production by the chemilumigenic probes lucigenin and luminol. Biochim. Biophys. Acta 1428, 1–12.

Li, L.S., Bey, E.A., Dong, Y., Meng, J., Patra, B., Yan, J., Xie, X.J., Brekken, R.A., Barnett, C.C., Bornmann, W.G., Gao, J., Boothman, D.A., 2011. Modulating endogenous NQO1 levels identifies key regulatory mechanisms of action of beta-lapachone for pancreatic cancer therapy. Clin. Cancer Res. 17, 275–285.

Liu, K.J., Miyake, M., Panz, T., Swartz, H., 1999. Evaluation of DEPMPO as a spin trapping agent in biological systems. Free Radic. Biol. Med. 26, 714–721.

Lu, W., Hu, Y., Chen, G., Chen, Z., Zhang, H., Wang, F., Feng, L., Pelicano, H., Wang, H., Keating, M.J., Liu, J., McKeehan, W., Luo, Y., Huang, P., 2012. Novel role of NOX in supporting aerobic glycolysis in cancer cells with mitochondrial dysfunction and as a potential target for cancer therapy. PLoS Biol. 10, e1001326.

Mosmann, T., 1983. Rapid colorimetric assay for cellular growth and survival: application to proliferation and cytotoxicity assays. J. Immunol. Methods 65, 55–63.

Neuzillet, C., Tijeras-Raballand, A., de Mestier, L., Cros, J., Faivre, S., Raymond, E., 2014. MEK in cancer and cancer therapy. Pharmacol. Ther. 141, 160–171.

Pardee, A.B., Li, Y.Z., Li, C.J., 2002. Cancer therapy with beta-lapachone. Curr. Cancer Drug Targets 2, 227–242.

Park, E.J., Choi, K.S., Kwon, T.K., 2011. beta-Lapachone-induced reactive oxygen species (ROS) generation mediates autophagic cell death in glioma U87 MG cells. Chem. Biol. Interact. 189, 37–44.

Pink, J.J., Planchon, S.M., Tagliarino, C., Varnes, M.E., Siegel, D., Boothman, D.A., 2000. NAD(P)H:Quinone oxidoreductase activity is the principal determinant of betalapachone cytotoxicity. J. Biol. Chem. 275, 5416–5424.

Ralph, S.J., Rodriguez-Enriquez, S., Neuzil, J., Saavedra, E., Moreno-Sanchez, R., 2010. The causes of cancer revisited: “mitochondrial malignancy” and ROS-induced oncogenic transformation — why mitochondria are targets for cancer therapy. Mol. Aspects Med. 31, 145–170.

Reinicke, K.E., Bey, E.A., Bentle, M.S., Pink, J.J., Ingalls, S.T., Hoppel, C.L., Misico, R.I., Arzac, G.M., Burton, G., Bornmann, W.G., Sutton, D., Gao, J., Boothman, D.A., 2005. Development of beta-lapachone prodrugs for therapy against human cancer cells with elevated NAD(P)H:quinone oxidoreductase 1 levels. Clin. Cancer Res. 11, 3055–3064.

Rota, C., Chignell, C.F., Mason, R.P., 1999. Evidence for free radical formation during the oxidation of 2′-7′-dichlorofluorescin to the fluorescent dye 2′-7′-dichlorofluorescein by horseradish peroxidase: possible implications for oxidative stress measurements. Free Radic. Biol. Med. 27, 873–881.

Shao, J., DeHaven, J., Lamm, D., Weissman, D.N., Malanga, C.J., Rojanasakul, Y., Ma, J.K., 2001. A cell-based drug delivery system for lung targeting: II. Therapeutic activities on B16–F10 melanoma in mouse lungs. Drug Deliv. 8, 71–76.

Siegel, D., Yan, C., Ross, D., 2012. NAD(P)H:quinone oxidoreductase 1 (NQO1) in the sensitivity and resistance to antitumor quinones. Biochem. Pharmacol. 83, 1033–1040.

Singh, K.K., 2006. Mitochondria damage checkpoint, aging, and cancer. Ann. N. Y. Acad. Sci. 1067, 182–190.

Timmins, G.S., Liu, K.J., Bechara, E.J., Kotake, Y., Swartz, H.M., 1999. Trapping of free radicals with direct in vivo EPR detection: a comparison of 5,5-dimethyl-1-pyrroline-Noxide and 5-diethoxyphosphoryl-5-methyl-1-pyrroline-N-oxide as spin traps for HO* and SO4*. Free Radic. Biol. Med. 27, 329–333.

Trachootham, D., Alexandre, J., Huang, P., 2009. Targeting cancer cells by ROS-mediated mechanisms: a radical therapeutic approach? Nat. Rev. Drug Discov. 8, 579–591.

Tronnier, M., Mitteldorf, C., 2014. Treating advanced melanoma: current insights and opportunities. Cancer Manag. Res. 6, 349–356.

Uyemura, S.A., Luo, S., Vieira, M., Moreno, S.N., Docampo, R., 2004. Oxidative phosphorylation and rotenone-insensitive malate- and NADH-quinone oxidoreductases in Plasmodium yoelii yoelii mitochondria in situ. J. Biol. Chem. 279, 385–393.

Villanueva, A., Hernandez-Gea, V., Llovet, J.M., 2013. Medical therapies for hepatocellular carcinoma: a critical view of the evidence. Nat. Rev. Gastroenterol. Hepatol. 10, 34–42.

Wallace, D.C., 2005. Mitochondria and cancer: Warburg addressed. Cold Spring Harb. Symp. Quant. Biol. 70, 363–374.

Wenner, C.E., 2012. Targeting mitochondria as a therapeutic target in cancer. J. Cell. Physiol. 227, 450–456.

Wu, L., Tang, Z.Y., Li, Y., 2009. Experimental models of hepatocellular carcinoma: developments and evolution. J. Cancer Res. Clin. Oncol. 135, 969–981.

Zang, L.Y., Misra, H.P., 1993. Generation of reactive oxygen species during the monoamine oxidase-catalyzed oxidation of the neurotoxicant, 1-methyl-4-phenyl-1,2,3,6-tetrahydropyridine. J. Biol. Chem. 268, 16504–16512.

Zhu, H., Jia, Z., Zhou, K., Misra, H.P., Santo, A., Gabrielson, K.L., Li, Y., 2009. Cruciferous dithiolethione-mediated coordinated induction of total cellular and mitochondrial antioxidants and phase 2 enzymes in human primary cardiomyocytes: cytoprotection against oxidative/electrophilic stress and doxorubicin toxicity. Exp. Biol. Med. (Maywood) 234, 418–429.